Journal of Medicinal Chemistry

Article

The Discovery and Optimization of 4,5-Diarylisoxazoles as Potent Dual Inhibitors of Pyruvate Dehydrogenase Kinase (PDHK) and Heat Shock Protein 90 (HSP90)

Tao Meng, Dadong Zhang, Zuoquan Xie, Ting Yu, Shuchao Wu, Min Huang, Mei-Yu Geng, and Jingkang Shen

J. Med. Chem., **Just Accepted Manuscript** • DOI: 10.1021/jm5010144 • Publication Date (Web): 10 Nov 2014

Just Accepted

The Discovery and Optimization of 4,5-Diarylisoxazoles as Potent Dual Inhibitors of Pyruvate Dehydrogenase Kinase (PDHK) and Heat Shock Protein 90 (HSP90)

Tao Meng[1#], Dadong Zhang[2#], Zuoquan Xie[2], Ting Yu[1], Shuchao Wu[2], Min Huang[2,], Meiyu Geng[2,*] and Jingkang Shen[1,*]*

[1] Division of Medicinal Chemistry, State Key Laboratory of Drug Research, Shanghai Institute of Materia Medica, Chinese Academy of Sciences, Shanghai 201203, People's Republic of China

[2] Division of Antitumor Pharmacology, State Key Laboratory of Drug Research, Shanghai Institute of Materia Medica, Chinese Academy of Sciences, Shanghai 201203, People's Republic of China

[#] These authors contributed equally to this work.

KEYWORDS: Pyruvate Dehydrogenase Kinases (PDHKs), Heat Shock Protein 90 (HSP90), 4,5-Diarylisoxazoles, Dual Inhibitors

ABSTRACT: Upregulation of pyruvate dehydrogenase kinase (PDHK) has been observed in a variety of cancers. Inhibition of PDHK offers an attractive opportunity

for the development of novel cancer therapies. To obtain novel PDHK inhibitors, we took advantage of the homology of the ATP-binding pocket between HSP90 and PDHK, and utilized 4,5-diarylisoxazole based HSP90 inhibitor for structural design. Our efforts led to the identification of **5k** that inhibited PDHK1 with an IC_{50} value of 17 nM, which however, showed marginal cellular activity. Further structural optimization resulted in compound **11a** with improved cellular activity which could effectively modulate the metabolic profile of cancer cells and led to the inhibition of cancer cell proliferation, evidenced by the increased oxidative phosphorylation and decreased glycolysis and associated oxidative stress. Our results suggested **11a** as an excellent lead compound and a favorable biological tool to further evaluate the therapeutic potential of PDHK and HSP90 dual inhibitors in the treatment of cancer.

INTRODUCTION

Most cancer cells feature a switch in metabolism from mitochondria-based glucose oxidation to cytoplasm-based glycolysis even under normoxia, also known as "Warburg effect". Such a metabolic profile, which is characterized by increased glycolysis and suppressed glucose oxidation, provides cancer cells with a proliferative advantage. Thus, to disrupt metabolic dependencies of cancer cells may represent a promising anticancer strategy. Indeed, increasing studies have suggested that targeting cancer-specific metabolic remodeling offer therapeutic opportunities in cancer treatment.[1]

Pyruvate dehydrogenase kinase (PDHK) is a mitochondrial enzyme that inhibits pyruvate dehydrogenase complex, a gatekeeper of glucose oxidation, and prevents

converting pyruvate to acetyl-CoA, the substrate for the Krebs'cycle. Activation of PDHK results in the uncoupling of glycolysis to glucose oxidation. Four isoforms, PDHK1, PDHK2, PDHK3 and PDHK4, have been identified in human cells, among which, PDHK1 is closely associated with cancer malignancy. PDHK1 is activated in various cancers such as lung cancer[2] and head and neck squamous cancer.[3] PDHK1 is transcriptionally regulated by oncogenes c-MYC and hypoxia-inducible factor1α (HIF1α)[4] to control metabolic and malignant phenotypes of cancer cells.[5] A recent study has also revealed that PDHK1 is commonly phosphorylated in human cancers by diverse oncogenic tyrosine kinases, which is important for promoting Warburg effect and tumor growth.[6] These evidence collectively suggest therapeutic opportunities arising from targeting PDHK in cancer therapy. In spite of the increasing number of reported PDHK inhibitors, such as dichloroacetate (DCA),[7] none of them has successfully entered clinical use.

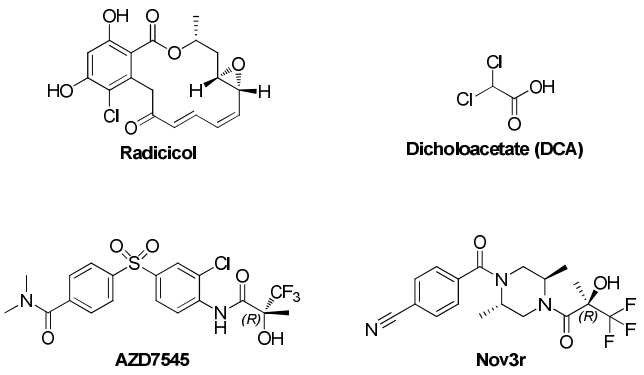

Figure 1. Known PDK inhibitors: Radicicol, Dichloroacetate (DCA), AZD7545, and Nov3r.

So far three major classes of PDHK inhibitors have been reported, which inhibit PDHK via different mechanisms. AZD7545 and Nov3r (Figure 1) contain the trifluoromethylpropanamide group and represent a class of PDHK inhibitors binding to the lipoyl-binding pocket of the enzymes.[8] DCA (Figure 1) inactivates PDHK kinase activity via binding to the helix bundle in the N-terminal.[9] Radicicol (Figure 1) belongs to a class of ATP-competitive inhibitor and inhibits kinase activity by binding to the ATP-binding pocket of PDHK, also known as GHKL domain.[10] Notably, GHKL domain has also been found in several other ATP-binding proteins, including histidine kinase, DNA gyrase B, topoisomerases,[11] and heat shock protein HSP90.[12] The folding of these GHKL domains is similar and over 50% of residues from PDHKs are superimposable with the corresponding residues in HSP90.[12b] This notion suggests that structure-activity relationship (SAR) information of HSP90 inhibitors could possibly guide the design of ATP-competitive PDHK inhibitors.[13]

In fact, two HSP90 inhibitors Radicicol and M77976 are known to bind weakly to the ATP binding site of PDHK3 and PDHK4, respectively. M77976 showed an IC_{50} of 648 μM against PDHK4,[14] whereas radicicol inhibited PDHK with a similar low potency of 400 μM (IC_{50}) against PDHK1 and 230 μM against PDHK3.[12b, 15] Structurally, M77976 belongs to the 4,5-diaryl-subtituted azole class. We speculated that the SAR for HSP90 might be translated to the activity for PDHK. Therefore, we examined AUY922, another HSP90 inhibitor belonging to 4,5-diaryl azole class but 20-fold more potent than M77976. As expected, the isoxazole core of AUY922 enabled enhanced activity against PDHK1 compared to M77976, with an IC_{50} of 11.9

μM. Meanwhile, we tested PDHK1 inhibitory activity of several known HSP90 inhibitors with different scaffolds, including purine analog (BIIB021), benzamide analog (SNX-2112) and resorcinol derivative (AT13387), but no active compounds were found at a concentration up to 30 μM.

Scheme 1. Design of PDHK inhibitors based on the combination of known PDHK4 and HSP90 inhibitors

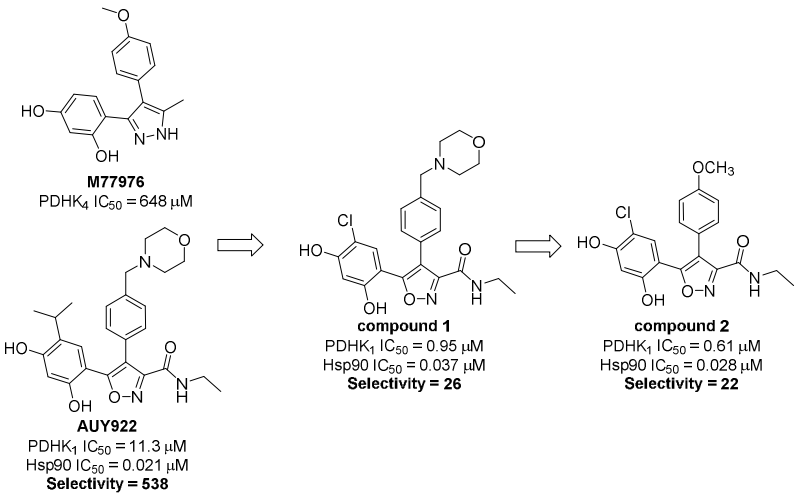

In spite of significantly improved potency against PDHK1, the potency of AUY922 against HSP90 appeared much higher (IC_{50} = 0.021 μM),[16] indicating that the affinity of oxazole-based AUY922 for PDHK1 was at least 500-fold lower than that for HSP90. In order to further increase the potency of PDHK inhibition, we synthesized two reported HSP90 inhibitors (compounds **1** and **2**) derived from M77976 and AUY922 (Scheme 1) and tested their activity in inhibiting PDHKs.[16] The replacement of iPr group (AUY922) with chloro (compound **1**) resulted in about 10-fold increase of the activity for PDHK1. Replacing the 4-morpholinomethyl group with 4-methoxyl

(compound **2**) slightly increased the PDHK1 potency and relative selectivity between PDHK1 and HSP90. Further inspection of this structure indicated that the amide group was suitable sites for modification. Thus, SAR studies were carried out by systemic molecular modulation on the compound **2**. The ethylamino group was replaced by incorporating solubilizing groups and meanwhile to probe the possibility of additional interaction with the amino acid side chains of PDHKs. Further optimization was centered on 3-acrylamide substituted isoxazole derivatives in order to improve the cellular activity (Scheme 2).

Scheme 2. Structural modification of compound 2

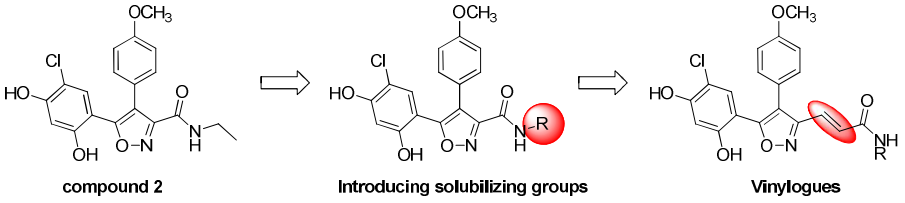

CHEMISTRY

The initial set of isoxazole derivatives **1** and **2**, as well as the key intermediate **3** (Scheme 3) were synthesized according to known literature procedures.[16] Hydrolyzing compound 3 with sodium hydroxide gave acid **4**. This acid was treated with oxalyl chloride to afford the corresponding acid chloride, which was used for subsequent acylations and boron trichloride-mediated deprotection to yield the amides **5a-e**. Acid **4** can also be coupled with 1-*N*-Boc-4-aminopiperidine to afford amide **12**, which was deprotected with 50% TFA to generate **13**. With intermediate **13** in hand, compound

5f-m were prepared by either acylation (**5f**), sulfonation (**5g**), ureation (**5h**) or reductive amination (**5i-m**) of the intermediate **13**. 3-Acrylamide substituted isoxazole derivatives **10a-i** were made using alternative procedures (Scheme 3) from the key intermediate **3** as well. Reduction of compound **3** under $LiAlH_4$ condition was utilized to afford the alcohol **6**, which was oxidized with activated MnO_2 to give the aldehyde **7**, followed by Horner-Wadsworth-Emmons reaction giving α,β-unsaturated ester **8**. This ester can be hydrolyzed with aqueous sodium hydroxide to afford acid **9**. Amidation with various amines, followed by debenzylation with boron trichloride provided the products **10a-i**. Some compounds of this class were made by a modified sequence, in which compounds **10b-i** were demethylated with boron tribromide to afford the phenolic compounds **11a-h** (Scheme 3).

Scheme 3. Conversion of Key Intermediate 3 to Isoxazole PDHK1 Inhibitors[a]

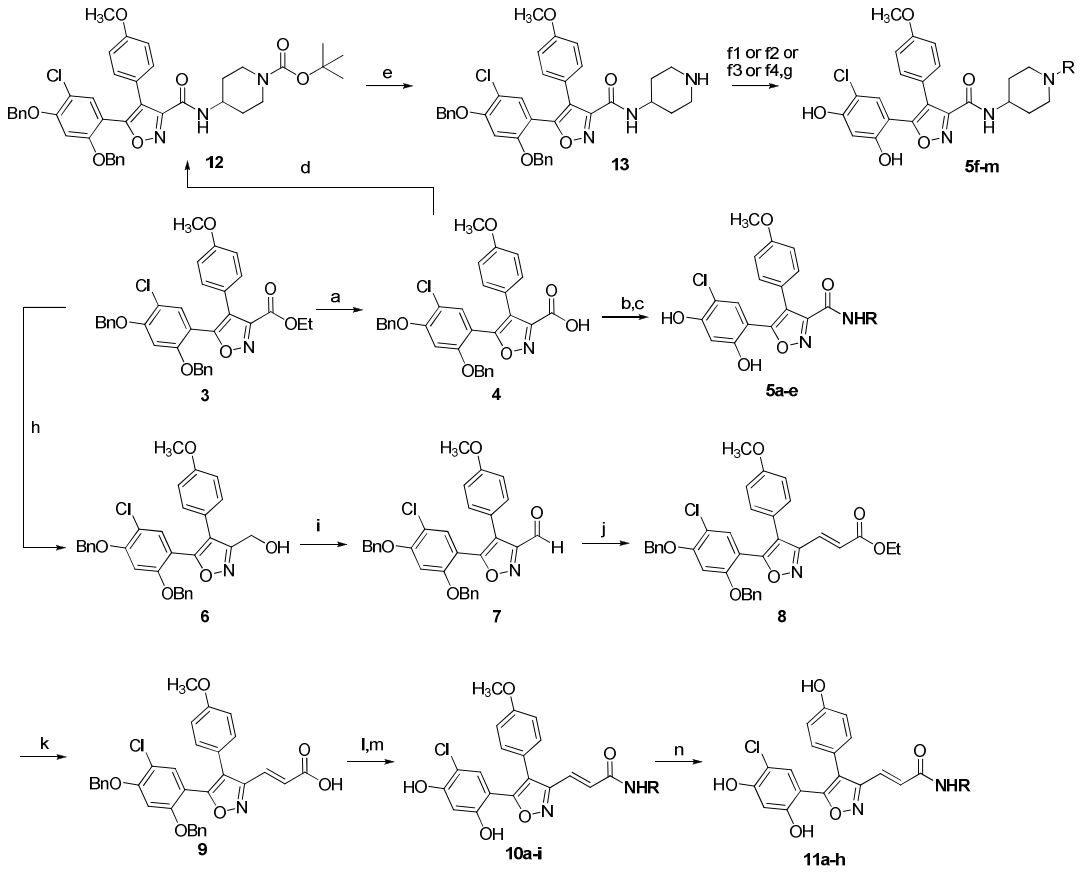

[a] Reagents and conditions: (a) NaOH, ethanol; (b) (i) Oxalyl chloride, DCM, 0 °C→rt; (ii) triethylamine, DCM, 0 °C→rt; (c) 1M BCl_3 in DCM, DCM; (d) (i) Oxalyl chloride, DMF, DCM; (ii) DIPEA, DCM; (e) CF_3COOH, 0 °C; (f1) acetyl chloride, triethylamine, DCM; (f2) methanesulfonyl chloride, triethylamine, DCM; (f3) isocyanatoethane, triethylamine, DCM; (f4) R-CHO, $NaBH(OAc)_3$, AcOH, 1,2-dichloroethane, 0 °C→rt; (g) 1M BCl_3 in DCM, DCM; (h) $LiAlH_4$, THF, 0 °C; (i) MnO_2, DCM; (j) 60% NaH, THF, 0 °C; (k) NaOH aq., ethanol; (l) RNH_2, EDCI, HOBt, triethylamine, DCM; (m) 1M BCl_3 in DCM; (n) 1M BBr_3 in DCM

RESULTS AND DISCUSSION

Therefore, a set of isoxazole amide substituted derivatives with different amino group were firstly synthesized and evaluated for their activity against PDHK. PDHK1 kinase activity was assessed using an enzyme-linked immunosorbent assay (ELISA) using recombinant PDHK1, and radicicol was used as a reference compound. HSP90 activity was assessed by luorescence polarization (FP) assay. All the compounds were evaluated at an initial concentration of 10 μM against PDHK1. Compounds showing over 50% inhibition rate at 10 μM were further evaluated to measure IC_{50} values. The PDHK1 inhibitory activities of the isoxazole amide derivatives (**5a-m**) were shown in Table 1. It was observed that the variation of the amino group affected the biological activity of the synthesized analogues. These compounds in general showed enhanced PDHK1 inhibitory activity in comparison to compound **2.** Four compounds were synthesized with the R-group selected as: 2,4-dichlorobenzylamine (**5a**), *N,N*-dimethylaniline (**5b**), 4-pyridyl (**5c**), 1-benzyl-*N*-methylpiperidin-4-amine (**5d**). It seemed the three benzylamine (**5a**) and aniline (**5b-c**) showed similar activities compare to **2** with ethylamino group. Interestingly, compound **5d** showed dramatic increase of PDHK1 inhibitory activity with IC_{50} of 25 nM, which suggested that the basic nitrogen may contribute to the high potency. To test this hypothesis, **5e**, a compound lack of the basic nitrogen was prepared. Indeed, **5e** lost the activity against PDHK1. Furthermore, the introduction of acetyl (**5f**), methylsulfonyl (**5g**) and ethylurea (**5h**) in the piperidine also dramatically decreased the activity compare to their parent compound **5d**, proving the importance of the basicity of the nitrogen in the piperidine ring. Further modification of 4-aminopiperidine revealed additional

gain of activity by replacing the benzyl group (**5d**) with various substituted phenyl ring, heterocycles, or alkyl groups. It suggested that the electronic withdrawn group (2,4-dichloro, **5j**) substituted phenyl ring decreased the activity, whereas the electronic donating group (4-methoxybenzyl substitution) retained or slightly increased the activity, with examples **5k** giving IC_{50} of 17 nM. 4-Pyridylmethyl (**5i**) or other alkyl substitutions (**5l**, **5m**) retained or slightly decreased the activity.

Table 1. Effects of Amides of 4,5-Diarylisoxazole on Inhibition of PDHK1 in ELISA assay[a]

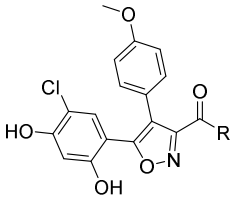

cpds	R Group	PDHK1 IC_{50} (μM)	HSP90 IC_{50} (μM)
5a	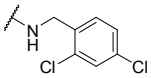	0.61 ± 0.03	1.600 ± 0.028
5b	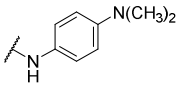	0.38 ± 0.02	0.091 ± 0.003
5c	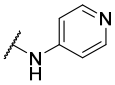	0.58 ± 0.15	0.154±0.022
5d	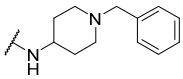	0.025 ± 0.005	0.036 ± 0.002
5e	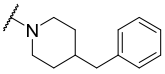	> 10	>10

5f	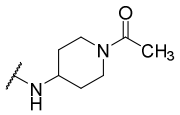	0.21 ± 0.02	0.025 ± 0.003
5g	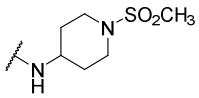	0.13 ± 0.07	0.045 ± 0.007
5h	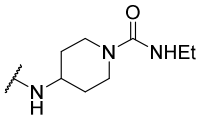	0.15 ± 0.01	0.020 ± 0.006
5i	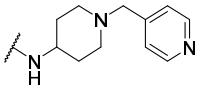	0.059 ± 0.018	0.015 ± 0.004
5j	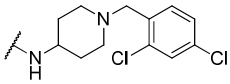	0.16 ± 0.07	0.127 ± 0.009
5k	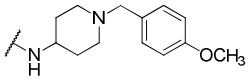	0.017 ± 0.004	0.016 ± 0.001
5l	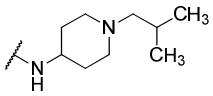	0.068 ± 0.023	0.023 ± 0.001
5m	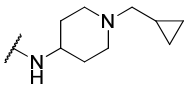	0.028 ± 0.007	0.039 ± 0.002

[a] The IC_{50} was calculated from two independent experimental measurements.

Table 2. Effects of Amides of New Vinylogs on Inhibition of PDHK1 in ELISA assay[a]

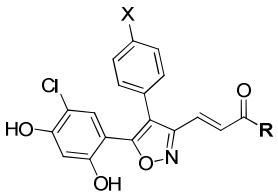

cpds	X	R	PDHK1 IC_{50} (μM)	HSP90 IC_{50} (μM)
10a	OCH_3	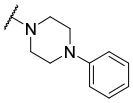	1.916 ± 0.631	0.677 ± 0.081
10b	OCH_3	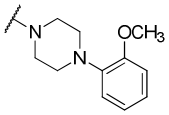	0.845 ± 0.200	0.596 ± 0.114
10c	OCH_3	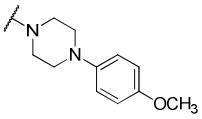	0.557 ± 0.027	0.700 ± 0.033
10d	OCH_3	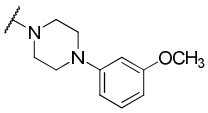	0.491 ± 0.094	0.718 ± 0.095
10e	OCH_3	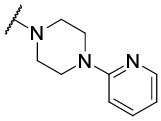	1.050 ± 0.129	0.215 ± 0.027
10f	OCH_3	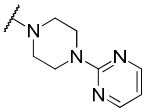	1.070 ± 0.471	0.208 ± 0.021
10g	OCH_3	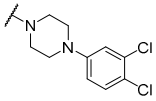	4.306 ± 2.362	4.232 ± 0.747
10h	OCH_3	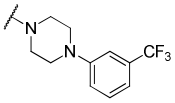	2.369 ± 0.514	2.255 ± 0.283
11a	OH	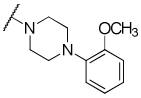	0.604 ± 0.054	0.512 ± 0.044
11b	OH	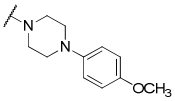	0.952 ± 0.073	0.576 ± 0.066
11c	OH	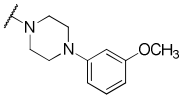	0.776 ± 0.168	0.666 ± 0.021

11d	OH	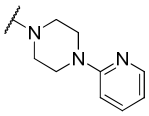	0.878 ± 0.313	0.357 ± 0.066
11e	OH	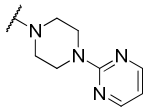	0.521 ± 0.113	0.338 ± 0.083
11f	OH	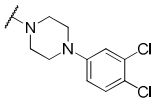	1.417 ± 0.436	3.939 ± 0.378
11g	OH	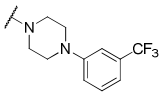	2.949 ± 0.721	1.859 ± 0.001

[a] The IC_{50} was calculated from two independent experimental measurements.

Our initial SAR exploration of the amide substituted isoxazoles led to the discovery of **5d** and **5k** as PDHK1 inhibitors with great potency. We then proceeded to evaluate the cellular activity of **5d** and **5k** in cancer cells. However, compounds **5d** and **5k** failed to show activities in the cellular assay (Figure 2C). We suspected that the lack of cellular activity was most likely attributed to the poor permeability of this structure class. We therefore tested permeability coefficient (P_{app}) of compound **5d and 5k** in Caco-2 cells (Table 5), which suggested that permeability was indeed a concern (Papp $< 1\times 10^{-6}$ cm/s). Next, we turned our attention to the vinylogues, which may change the conformation of these compounds and improve permeability.[17] Based on the above SAR information, 4-aminopiperidine was replaced with N-acrylamide substituted piperizines. Data presented in Table 2 showed that the new vinylogs (**10a-h** and **11a-g**) all exhibited moderate inhibitory activity against PDHK1. The data

indicated the substituents on the aromatic ring of the arylpiperizine had some effect on their activity against PDHK1. In general, the introduction of EWGs on the phenyl ring decreased activity compared with the EDGs substituted phenyl derivative or electronic rich aromatic rings. The compounds **10b-d** having 2-, 3- and 4-methoxypheyl at R position showed improved activity compared with the compound **10a** with non-substituted phenyl ring, whereas, compounds **10g** and **10h** bearing the EWGs such as 3,4-dichloro, 3-trifluoromethyl group showed decreased activity. Compounds **10e-g** containing the heterocyclic substituted piperizine also showed similar PDHK1 inhibitory activities. Demethylation of compounds **10b-i** afforded the corresponding compounds **11a-h.** As shown in Table 2, most of the phenolic derivatives retained the inhibitory activity and the SAR showed similar pattern as their parent compounds. We then measured the cellular activity of these compounds (compounds **11a-h**, and compound **5k)** using a high content analysis, which examined the impact on the downstream PDH phosphorylation. As shown in Figure 2A-B, most of these scaffolds showed good cellular activity. Compounds **10b**, **10c**, **10d**, **10e**, **10f**, **11a**, **11b**, **11c**, **11d** and **11e** effectively decreased phosphorylation of both S293 and S232. The enzymatically less potent compounds **11g** only slightly decreased the phosphorylation of S232 but not that of S293. The cellular activity of the three most potent compounds **10f**, **11a** and **11c** were further verified using immunoblotting analysis, where 10 μM of each compound almost abolished PDH phosphorylation at both sites (Figure 2C).

We also compared the activity of these compounds on PDHK1 and HSP90, which overall showed a comparable inhibition against the two enzymes (Table 1 and Table 2). For instance, compounds **10f**, **11a** and **11c** showed at least 10-fold decrease than compounds **5d**, **5k** and **5m** in both HSP90 and PDHK1 inhibition at the molecular level, which may be explained by the similar ATP binding affinity of PDHK and HSP90. ATP binding affinity for HSP90 is at hundred micromolar level, with a Km range from 770 to 840 μM [18, 19], comparable to ATP binding affinity to PDHK [20]. At the cellular level, both compound **sets** exhibited apparent cellular impacts on HSP90 activity, as indicated by the dramatic down-regulation of HSP90 client proteins such as AKT, HER2 and c-MET, and some up-regulation of its client protein HSP70 (Figure 2C). Together, compounds **11a**, **11c** and **10f** exhibited apparent inhibition on PDHK1 besides its inhibition HSP90, in spite of a decrease of activity on HSP90 when compared to compounds **5d**, **5k** and **5m**.

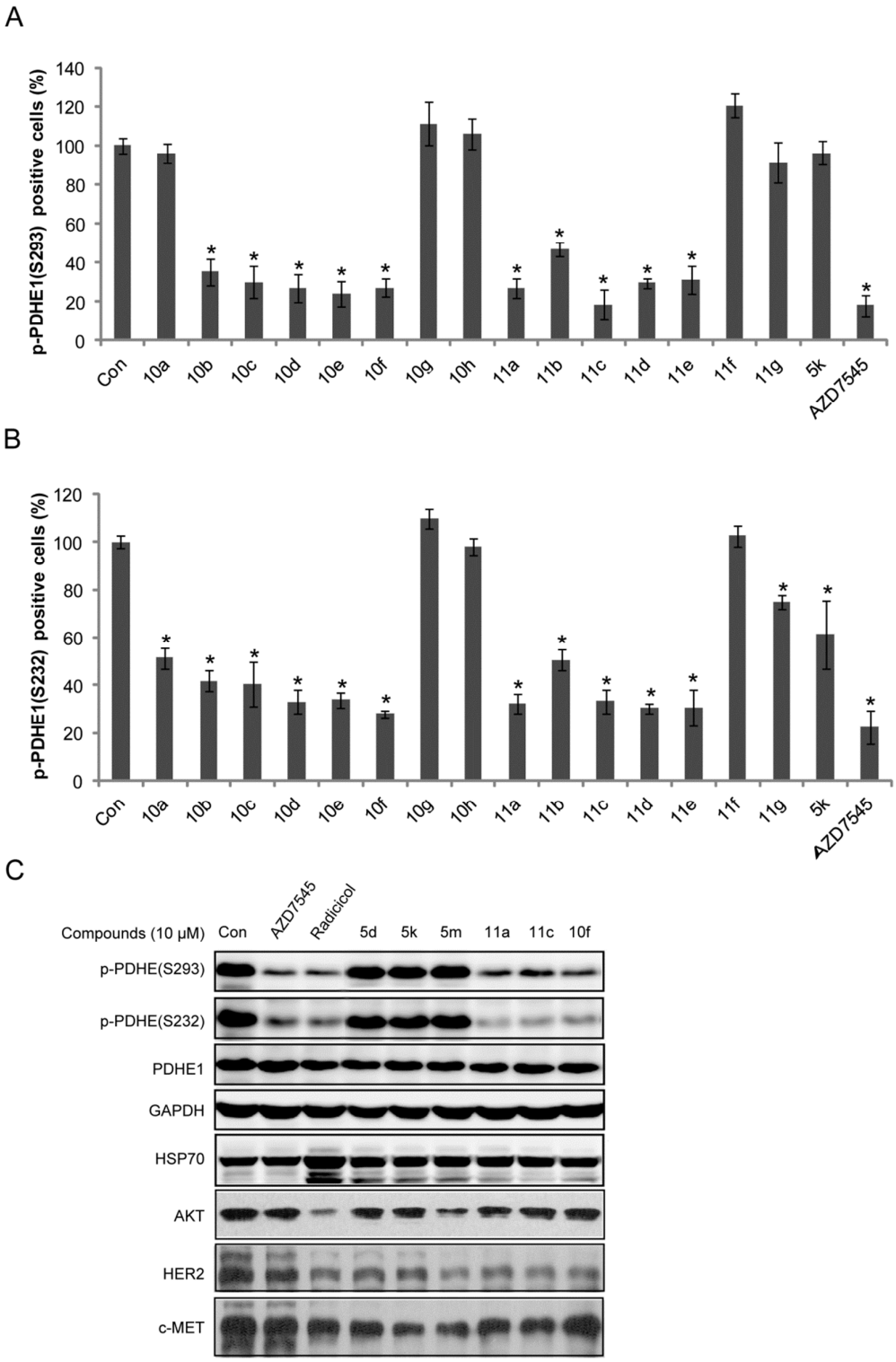

Figure 2. Cellular activity of compounds on PDHKs inhibition; A, B) NCI-H1299 cells were treated with indicated compounds for 12 h (10 μM); AZD7545 was a

positive contro1. The decrease of PDH phosphorylation (S293 and S232) was a reflection of PDHK inhibition, and was determined by high content analysis, in which cells were defined as positive or negative according to their relative fluorescence intensity compared to the average intensity; The data were expressed as the percent of positive cells versus total cells; C) Activity of compounds were determined by immunoblotting analysis. AZD7545 and radiciciol were used as positive controls; *P<0.05, versus untreated control group.

We then asked whether the enhanced cellular potency of was caused by improved cell membrane permeability. P_{app} of selected compounds **10f**, **11a** and **11c** was measured and compared with that of **5d** and **5k**. Consistent with their cellular activity, compounds **5d** and **5k** showed low permeability ($P_{app} < 1\times 10^{-6}$ cm/s) and high efflux ratio (Table 3), whereas compounds **10f**, **11a** and **11c** exhibited moderate permeability ($P_{app} > 5 \times 10^{-6}$ cm/s) and low efflux ratio (Table 3). This result indicated that the compromised cellular activity of compound **5d** and **5k** may result from the low cell membrane permeability and high efflux ratio. Presumably, compounds pass through the additional barrier of mitochondria membranes may have much more impacts on their activity against PDHK1 at cellular level, as PDHK1 is located in mitochondrial which is different from HSP90 that localized at cytosol and easy to reach for compounds. Therefore, compounds **10f**, **11a** and **11c** were supposed to be easier to reach mitochondrial PDHK, and would be considered in further optimization.

Table 3. Permeability of selected compounds

cpds	Papp (× 10^{-6} cm/s) (AP→BL)	Papp (× 10^{-6} cm/s) (BL→AP)	Efflux ratio
5d	0.936 ± 0.029	9.41 ± 0.27	10.05
5k	0.962 ± 0.012	8.70 ± 0.21	9.04
10f	6.90 ± 0.03	5.09 ± 0.03	0.74
11a	11.2 ± 0.4	15.5 ± 0.9	1.38
11c	6.54 ± 0.14	15.0 ± 0.2	2.29

To gain a better understanding of PDHK inhibitory activity and associated metabolic modulation efficacy of the compounds, compound **11a,** the most potent compound on both enzymatic and cell-based assays, was selected as a representative. First, we determined the mode of action of the compound. As a compound derived from the ATP competitive inhibitors, the ATP competitiveness of the compound was determined using Lineweaver-Burk plot. Radicicol, an ATP competitive inhibitor of PDHK, was selected as a positive control. The result showed that compound **11a** inhibited PDHK1 activity in an ATP-dependent manner, with curves crossing at the y-intercept (Figure 3A), suggesting that compound **11a** competed with ATP to access the ATP-binding pocket of PDHK. To examine the selectivity of compound **11a** on

PDHK isozymes, the inhibitory activity against at PDHK2, PDHK3 and PDHK4 was determined as well. The IC_{50} against PDHK2, PDHK3 and PDHK4 was 1.126 μM, 5.336 μM and 1.743 μM respectively (Figure 3B), showing that compound **11a** is pan-PDHKs inhibitor, with a less potency on other isozymes in contrast to PDHK1. The cellular potency of **11a** was evaluated in NCI-H1299 non-small lung cancer cell cline. Cells were treated with various concentrations of **11a** for 12 h. The PDH phosphorylation at both S293 and S232 sites were significantly decreased in a concentration-dependent manner, as well as the increase of HSP70 and decrease of AKT (Figure 3C). The cellular activity of compound **11a** on phosphorylation of PDH was further evaluated by high content analysis (Figure 3D, 3E). Compound **11a** showed a similar potency as that of AZD7545 and was nearly 1000 fold more potent than DCA. These results demonstrated that compound **11a** is a novel ATP competitive inhibitor of PDHK, with potent activity at both molecular and cellular levels.

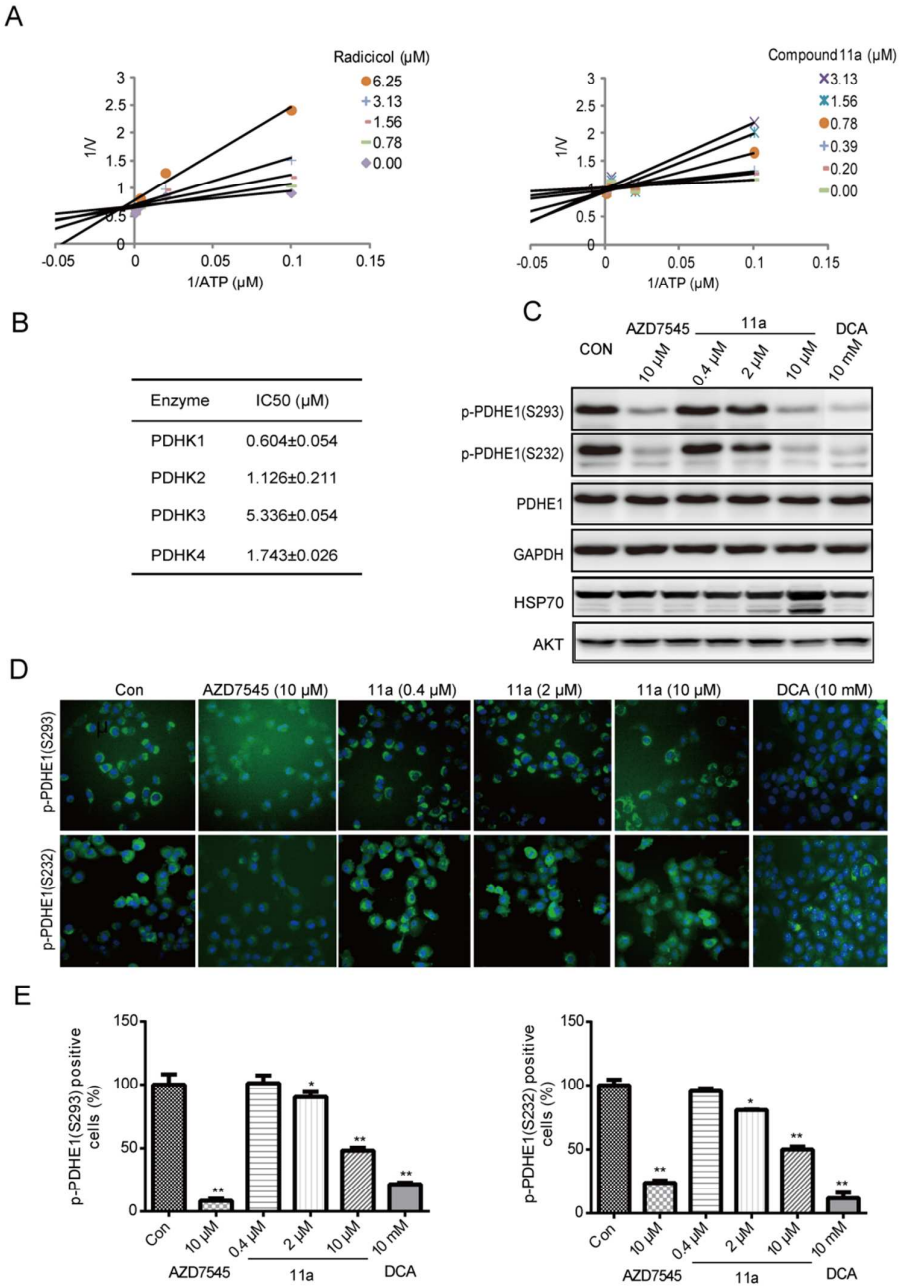

Enzyme	IC50 (μM)
PDHK1	0.604±0.054
PDHK2	1.126±0.211
PDHK3	5.336±0.054
PDHK4	1.743±0.026

Figure 3. Characterization of inhibition of compound 11a on PDHK; A) ATP competitiveness of compound **11a** on PDHK1 that determined by Lineweaver-Burk plot, showing compound **11a** is an ATP competitive inhibitor on PDHK1; B) Inhibitory activity of **11a** on PDHK isozymes, as determined by ELISA assay; C) Inhibitory activity of compound **11a** on PDH phosphorylation in NCI-H1299 cells as

determined by western blot; D) Effect of 11a on PDH phosphorylation (S293 and S232), HSP70 and AKT in NCI-H1299 cells as determined by high content analyzer, AZD7545 and DCA were positive controls, the magnification is 200×; E) Quantitative analysis of Figure 3D, cells were defined as positive cells and negative cells according the fluorescence intensity with above or below the averaged intensity, the data was expressed as the percent of positive cells verses total cells; *P<0.05, as compared to control group.

Inhibition of PDHK activity results in the activation of PDH, leading to a switch of pyruvate consumption from lactate production to oxidative phosphorylation. As shown in Figure 4A, lactate production was significantly decreased by compound **11a** at 10 μM in NCI-H1299 cancer cells after 12 h of treatment, showing a similar potency as 10 mM of DCA. The metabolic modulatory effect of compound **11a** was evaluated by measuring oxygen consumption rate (OCR) and extracellular acidification (ECAR). ECAR was decreased by compound **11a,** which is consistent with the lactate production change (Figure 2B). Unexpectedly, OCR was decreased as well (Figure 2C), which may resulted from the simultaneous Hsp90 inhibition that overrides the metabolic effect. As such, we expanded to other well-known HSP90 inhibitors, including 17-DMAG, PU-H71, BIIB 021, SNX-2112 and STA-9090. All these compounds led to decreased OCR (Supplementary Figure S1A). We further compared the ratio of OCR/ECAR. OCR/ECAR was dramatically increased by

compound 11a (Figure 4D, Supplementary Figure S2) but not by HSP90 specific inhibitors (Figure 4D, Supplementary Figure S1B). Thus, compound 11a is distinct from HSP90 inhibitors by increasing the ratio of OCR/ECAR, which may result from concurrent PDHK and HSP90 inhibition.

In line with accelerated oxidative phosphorylation, compound **11a** increased the production of reactive oxygen species (ROS), a byproduct and indicator of oxidative phosphorylation. (Figure 4C). We also tested the anti-proliferative effect of compound **11a** in NCI-H1299 cells using CCK8 assay. Compound **11a** dose-dependently inhibited NCI-H1299 cell proliferation with an IC_{50} of 9.21 ± 1.33 μM (Figure 4D). As compound 11a also has inhibitory activity on HSP90, the anti-proliferation effect may result from its impacts on both PDHK and HSP90.

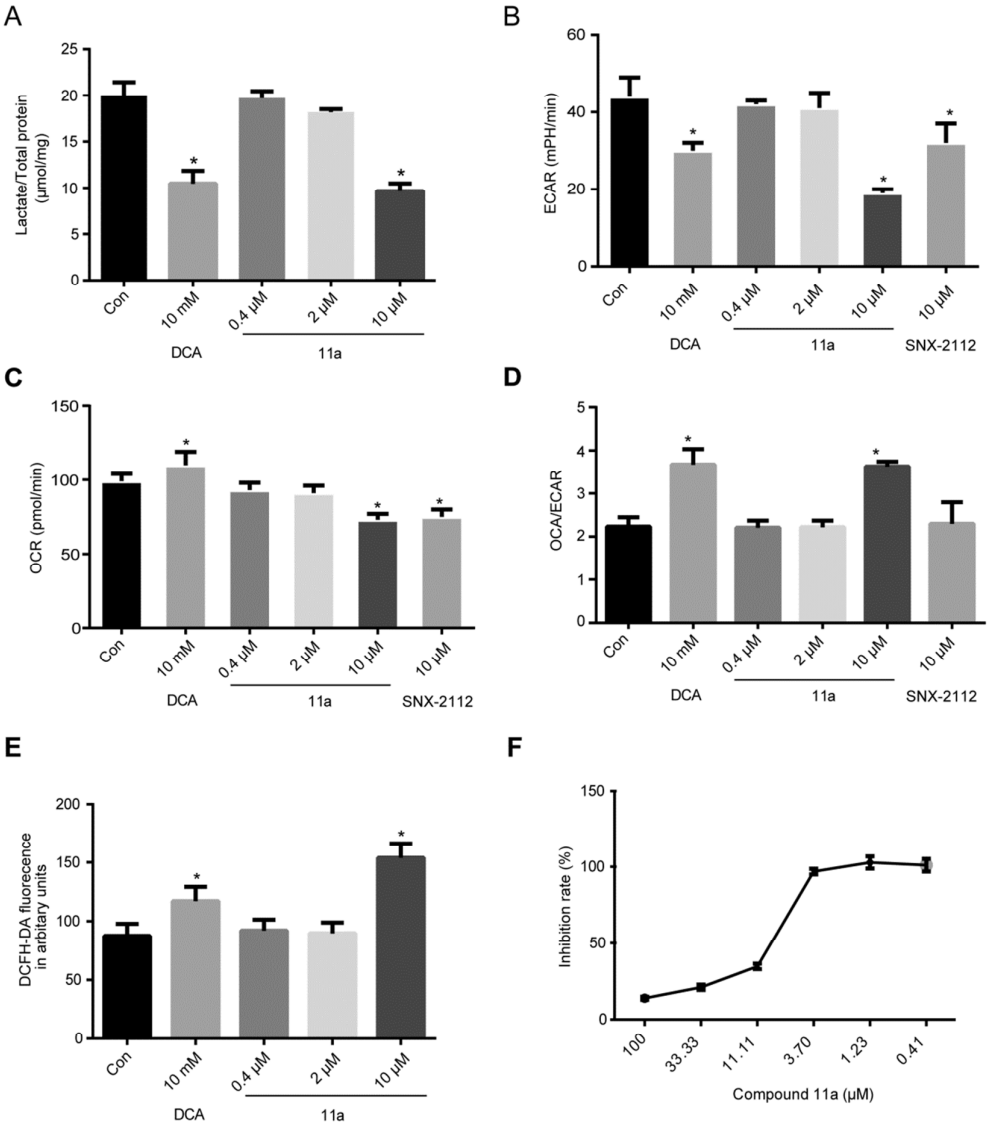

Figure 4. Effect of compound 11a on cell metabolism and proliferation; A) NCI-H1299 cells was treated with various concentration of compound **11a** for 12 h, lactate production was significantly decreased by compound **11a** at 10 μM, DCA was used as a positive control; B) ECAR was significantly increased by compound **11a** at 10 μM (12 h), DCA (10 mM) and SNX-2112; C) OCR was significantly increased by DCA (10 mM), but decreased by compound **11a** at 10 μM (12 h) as well as SNX-2112; B) Ratio of ECAR/OCR was significantly increased by compound **11a** at

10 μM (12 h) as well as by DCA (10 mM), but not SNX-2112; E) Reactive oxygen species production was significantly increased by compound **11a** at 10 μM; F) compound **11a** inhibited NCI-H1299 cell proliferation with a IC_{50} of 9.21±1.33 (μM), as measured by CCK8;*P<0.05, as compared to control group.

In addition to NCI-H1299 cells, we further expanded to other cancer cell lines derived from different tissues to verify the anticancer activity of compound **11a** via metabolic modulation. Two lung cancer cell lines A549 and H460, and colon cancer cell lines HCT116 and breast cancer cell lines MDA-MB-231 were selected. The results showed that compound **11a** effectively decreased PDH phosphorylation at both S293 and S232 sites in a concentration-dependent manner and accordingly the lactate production in parallel (Figure 5) in all tested cell lines.

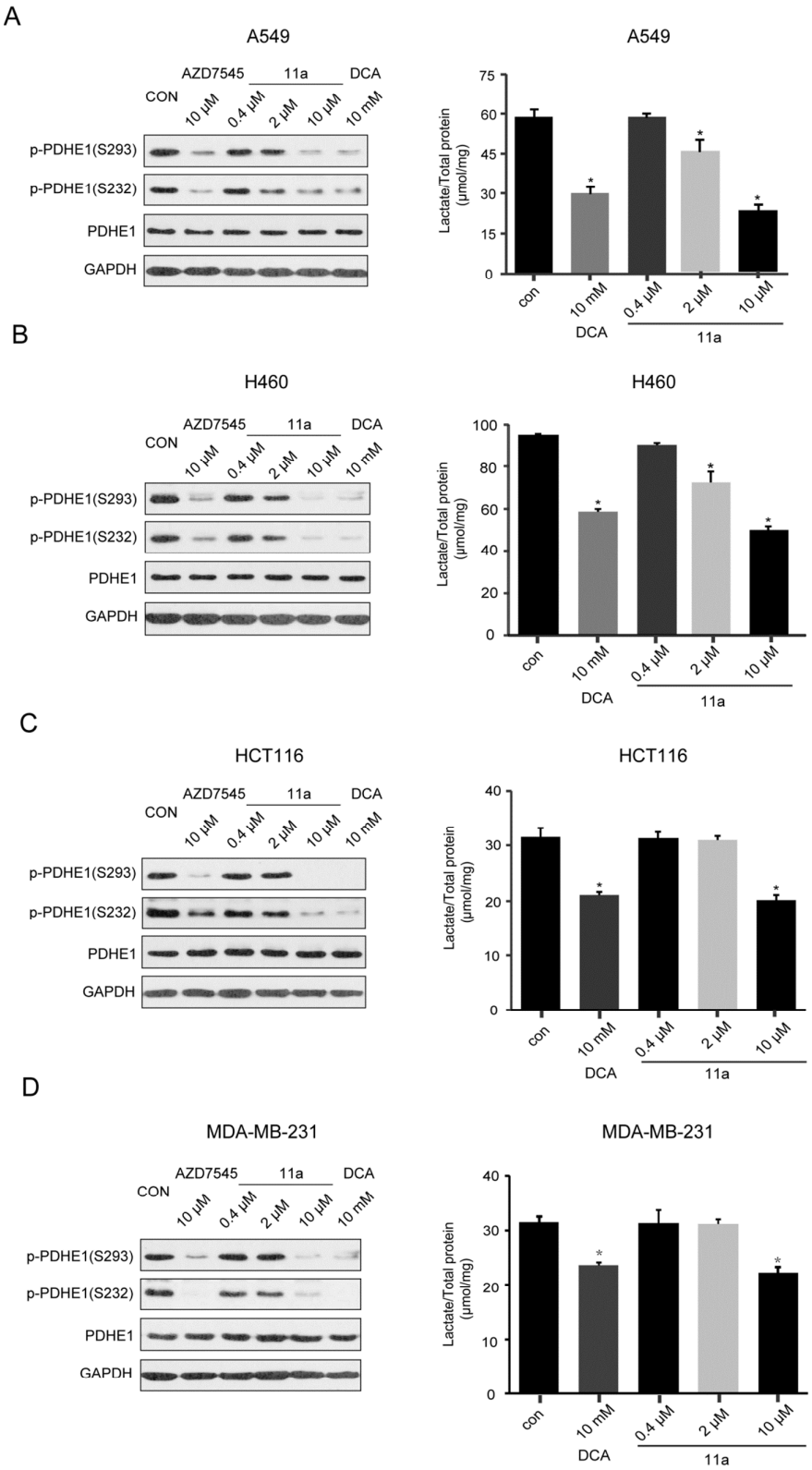
A
A549
AZD7545
11a
DCA
CON
10 μM
0.4 μM
2 μM
10 μM
10 mM
p-PDHE1(S293)
p-PDHE1(S232)
PDHE1
GAPDH
Lactate/Total protein (μmol/mg)
con
10 mM
0.4 μM
2 μM
10 μM
DCA
11a
B
H460
C
HCT116
D
MDA-MB-231

Figure 5. Activity of compound 11a in cancer cell lines; Inhibitory activity of compound **11a** on PDH phosphorylation (12 h) and lactate production (12 h) in A549 cells (A), H460 cells (B), HCT116 cells (C) and MDA-MB-231 cells (D); *P<0.05, as compared to control group.

CONCLUSIONS

Starting with the HSP90 inhibitors, we developed several 3-amide substituted isoxazole derivatives as potent inhibitors of PDHK and HSP90. To improve cellular potency of this series, we designed their vinylogues aiming at achieving balanced PDHK in vitro potency and physicochemical properties aiding cell penetration. Among those, compound **11a** was found to be an excellent lead compound as well as a favorable biological tool to further evaluate the therapeutic potential of dual PDHK and HSP90 inhibitor in the treatment of cancer.

EXPERIMENTAL SECTION

Chemistry: General Methods. ^{1}H NMR (400 MHz) spectra were recorded by using a Varian Mercury-400 high performance digital FT-NMR spectrometer with tetramethylsilane (TMS) as an internal standard. ^{13}C NMR (100 or 125 MHz) spectra were recorded by using a Varian Mercury-400 high performance digital FT-NMR spectrometer or Varian Mercury-500 high performance digital FT-NMR spectrometer. Abbreviations for peak patterns in NMR spectra are the following: br = broad, s =

singlet, d = doublet, and m = multiplet. Low-resolution mass spectra were obtained with a Finnigan LCQ Deca XP mass spectrometer using a CAPCELL PAK C18 (50 mm × 2.0 mm, 5 μm) or an Agilent ZORBAX Eclipse XDB C18 (50 mm × 2.1 m, 5 μm) in positive electrospray mode. High-resolution mass spectra were recorded by using a Finnigan MAT-95 mass spectrometer or an Agilent Technologies 6224 TOF mass spectrometer. Purity of all compounds was determined by analytical Gilson high-performance liquid chromatography (HPLC) using a YMC ODS3 column (50 mm × 4.6 mm, 5 μm). Conditions were as follows: CH_3CN/H_2O eluent at 2.5 mL min−1 flow [containing 0.1% trifluoroacetic acid (TFA)] at 35 °C, 8 min, gradient 5% CH3CN to 95% CH_3CN, monitoring by UV absorption at 214 and 254 nm. The purities of all biologically evaluated compounds are > 95%. All solvents and reagents were used directly as obtained commercially unless otherwise noted. All air and moisture sensitive reactions were carried out under an atmosphere of dry argon with heat-dried glassware and standard syringe techniques. Melting points were determined using a SGW X-4 hot stage microscope and are uncorrected.

(*E*)-3-(5-(5-chloro-2,4-dihydroxyphenyl)-4-(4-methoxyphenyl)isoxazol-3-yl)-1-(4-phenylpiperazin-1-yl)prop-2-en-1-one (**10a**). **9** (150mg, 0.26mmol) in DCM was added EDCI (60 mg, 0.32 mmol) and HOBt (43 mg, 0.32 mmol), then triethylamine (110 μL, 0.79 mmol) and 1-phenylpiperazine (43 mg, 0.26 mmol) was added, the mixture was stirred at RT overnight. The resulting mixture was washed with water, saturate $NaHCO_3$, brine, and dried with Na_2SO_4. After removal of the solvent, the

brown solid was dissolved in DCM, then 1M BCl_3 in DCM (1.3 mL, 1.3 mmol) was added, the mixture was stirred at RT for 6 h. Removed the solvent and the product was purified via silica gel chromatography(DCM/MeOH) to give a yellow solid (77.3 mg, 56% yield, HPLC purity: 99); mp 244 – 248 ^{o}C; ^{1}H NMR (400 MHz, Acetone-d_6) δ 7.40 (d, J = 15.6 Hz, 1H), 7.29 - 7.21 (m, 5H), 7.18, (d, J = 15.6 Hz, 1H), 7.04 - 6.98 (m, 4H), 6.84 (t, J = 7.3 Hz, 1H), 6.69 (s, 1H), 3.83 (s, 3H), 3.81 - 3.68 (m, 4H), 3.25 - 3.15 (m, 4H); HRMS calcd for $C_{29}H_{25}ClN_3O_5$ ([M - H]$^-$): 530.1488, found: 530.1477.

(*E*)-3-(5-(5-chloro-2,4-dihydroxyphenyl)-4-(4-methoxyphenyl)isoxazol-3-yl)-1-(4-(2-methoxyphenyl)piperazin-1-yl)prop-2-en-1-one (**10b**). Compound **10b** was prepared according the described procedure of **10a**, to give **10b** as yellow solid (81.7 mg, 56% yield, HPLC purity: 98); mp 195 – 197 ^{o}C; ^{1}H NMR (400 MHz, Acetone-d_6) δ 7.40 (d, J = 15.6 Hz, 1H), 7.32 - 7.23 (m, 3H), 7.17 (d, J = 15.6 Hz, 1H), 7.03 - 6.88 (m, 6H), 6.68 (s, 1H), 3.87 (s, 3H), 3.83 (s, 3H), 3.79 - 3.74 (m, 2H), 3.70 - 3.65 (m, 2H), 3.07 - 3.01 (m, 4H); HRMS calcd for $C_{30}H_{27}ClN_3O_6$ ([M - H]$^-$): 560.1594, found: 560.1588.

(*E*)-3-(5-(5-chloro-2,4-dihydroxyphenyl)-4-(4-methoxyphenyl)isoxazol-3-yl)-1-(4-(4-methoxyphenyl)piperazin-1-yl)prop-2-en-1-one (**10c**). Compound **10c** was prepared according the described procedure of **10a**, to give **10c** as yellow amorphous solid (87.5 mg, 60% yield, HPLC purity: 96); ^{1}H NMR (400 MHz, Acetone-d_6) δ 7.39

(d, J = 15.6 Hz, 1H), 7.29 - 7.20 (m, 4H), 7.17 (d, J = 15.6 Hz, 1H), 7.01 - 6.95 (m, 3H), 6.88 - 6.83 (m, 2H), 6.80 (s, 1H), 3.82 (s, 3H), 3.78 - 3.73 (m, 5H), 3.69 - 3.66 (m, 2H), 3.09 - 3.02 (m, 4H); $C_{30}H_{27}ClN_3O_6$ ([M - H]$^-$): 560.1594, found: 560.1583.

(*E*)-3-(5-(5-chloro-2,4-dihydroxyphenyl)-4-(4-methoxyphenyl)isoxazol-3-yl)-1-(4-(3-methoxyphenyl)piperazin-1-yl)prop-2-en-1-one (**10d**). Compound **10d** was prepared according the described procedure of **10a**, to give **10d** as yellow solid (84.6 mg, 58% yield, HPLC purity: 100); mp 229 – 230 ^oC; ^1H NMR (400 MHz, Acetone-d_6) δ 7.39 (d, J = 15.6 Hz, 1H), 7.29 - 7.23 (m, 3H), 7.20 - 7.12 (m, 2H), 7.04 - 6.96 (m, 2H), 6.67 (s, 1H), 6.59 (dd, J = 8.3, 2.3 Hz, 1H), 6.54 (t, J = 2.3 Hz, 1H), 6.43 (dd, J = 8.2, 2.3 Hz, 1H), 3.83 (s, 3H), 3.78 - 3.67 (m, 7H), 3.23 - 3.17 (m, 4H); HRMS calcd for $C_{30}H_{27}ClN_3O_6$ ([M - H]$^-$): 560.1594, found: 560.1588.

(*E*)-3-(5-(5-chloro-2,4-dihydroxyphenyl)-4-(4-methoxyphenyl)isoxazol-3-yl)-1-(4-(pyridin-2-yl)piperazin-1-yl)prop-2-en-1-one (**10e**). Compound **10e** was prepared according the described procedure of **10a**, to give **10e** as yellow solid (77.5 mg, 56% yield, HPLC purity: 100); mp 251 – 255 ^oC; ^1H NMR (400 MHz, Acetone-d_6) δ 8.15 (m, 1H), 7.55 (m, 1H), 7.40 (d, J = 15.6 Hz, 1H), 7.28 - 7.25 (m, 3H), 7.19 (d, J = 15.6 Hz, 1H), 7.03 - 6.99 (m, 2H), 6.84 (d, J = 8.6 Hz, 1H), 6.68 - 6.65 (m, 2H), 3.84 (s, 3H), 3.78 - 3.55 (m, 8H); HRMS calcd for $C_{28}H_{26}ClN_4O_5$ ([M+H]$^+$): 533.1586, found: 533.1592.

(*E*)-3-(5-(5-chloro-2,4-dihydroxyphenyl)-4-(4-methoxyphenyl)isoxazol-3-yl)-1-(4-(pyrimidin-2-yl)piperazin-1-yl)prop-2-en-1-one (**10f**). Compound **10f** was prepared according the described procedure of **10a**, to give **10f** as yellow amorphous solid (76.2 mg, 55% yield, HPLC purity: 95); ^{1}H NMR (400 MHz, Acetone-d_6) δ 8.38 (d, J = 4.7 Hz, 2H), 7.40 (d, J = 15.6 Hz, 1H), 7.29 – 7.24 (m, 3H), 7.19 (d, J = 15.6 Hz, 1H), 7.03 - 6.99 (m, 2H), 6.67 (s, 1H), 6.64 (t, J = 4.7 Hz, 1H), 3.89 - 3.81 (m, 7H), 3.73 - 3.61 (m, 4H); HRMS calcd for $C_{27}H_{23}ClN_5O_5$ ([M - H]$^-$): 532.1393, found: 532.1388.

(*E*)-3-(5-(5-chloro-2,4-dihydroxyphenyl)-4-(4-methoxyphenyl)isoxazol-3-yl)-1-(4-(3,4-dichlorophenyl)piperazin-1-yl)prop-2-en-1-one (**10g**). Compound **10g** was prepared according the described procedure of **10a**, to give **10g** as yellow amorphous solid (93.4 mg, 60% yield, HPLC purity: 100); ^{1}H NMR (400 MHz, Acetone-d_6) δ 7.39 (dd, J = 12.3, 3.3 Hz, 2H), 7.28 - 7.23 (m, 3H), 7.19 (d, J = 15.6 Hz, 1H), 7.19 (d, J = 15.6 Hz, 1H), 7.02 - 6.97 (m, 3H), 6.67 (s, 1H), 3.38 (s, 3H), 3.80 - 3.70 (m, 4H), 3.33 - 3.26 (m, 4H); HRMS calcd for $C_{29}H_{23}Cl_3N_3O_5$ ([M - H]$^-$): 598.0709, found: 598.0703.

(*E*)-3-(5-(5-chloro-2,4-dihydroxyphenyl)-4-(4-methoxyphenyl)isoxazol-3-yl)-1-(4-(3-(trifluoromethyl)phenyl)piperazin-1-yl)prop-2-en-1-one (**10h**). Compound **10h** was prepared according the described procedure of **10a**, to give **10h** as yellow solid (95.0 mg, 61% yield, HPLC purity: 97); mp 188 – 190 ^{o}C; ^{1}H NMR (400 MHz,

Acetone-d_6) δ 7.46 (m, 1H), 7.40 (d, J = 15.6 Hz, 1H), 7.30 - 7.24 (m, 5H), 7.20 (d, J = 15.6 Hz, 1H), 7.13 (d, J = 7.1 Hz, 1H), 7.02 - 6.97 (m, 2H), 6.67 (s, 1H), 3.85 - 3.72 (m, 7H), 3.38 - 3.29 (m, 4H); HRMS calcd for $C_{30}H_{24}ClF_3N_3O_5$ ([M - H]$^-$): 598.1362, found: 598.1357

(*E*)-3-(5-(5-chloro-2,4-dihydroxyphenyl)-4-(4-hydroxyphenyl)isoxazol-3-yl)-1-(4-(2-methoxyphenyl)piperazin-1-yl)prop-2-en-1-one (11a). **10b** (50 mg, 0.09mmol) was dissolved in 5 mL of DCM, then 1M BBr_3 in DCM (1.3 mL, 1.3 mmol) was added, the mixture was stirred at RT for 6h. Removed the solvent and the product was purified via silica gel chromatography(DCM/MeOH) to give a yellow solid (27.6 mg, 56% yield, HPLC purity: 98); mp 219 – 223 ^oC; ^1H NMR (400 MHz, Acetone-d_6) δ 9.21 (brs, 1H), 8.91 (brs, 1H), 8.63 (brs, 1H), 7.41 (d, J = 15.6 Hz, 1H), 7.26 (s, 1H), 7.20 - 7.14 (m, 2H), 7.03 - 6.87 (m, 7H), 6.68 (s, 1H), 3.87 (s, 3H), 3.79 - 3.65 (m, 4H), 3.07 - 3.01 (m, 4H); HRMS calcd for $C_{29}H_{25}ClN_3O_6$ ([M - H]$^-$): 546.1437, found: 546.1426.

(*E*)-3-(5-(5-chloro-2,4-dihydroxyphenyl)-4-(4-hydroxyphenyl)isoxazol-3-yl)-1-(4-(4-methoxyphenyl)piperazin-1-yl)prop-2-en-1-one (**11b**). Compound **11b** was prepared according the described procedure of **11a**, to give **11b** as yellow amorphous solid (29.5 mg, 60% yield, HPLC purity: 99); ^1H NMR (400 MHz, Acetone-d_6) δ 7.40 (m, 1H), 7.26 (m, 1H), 7.20 - 7.14 (m, 3H), 7.00 - 6.96 (m, 2H), 6.93 - 6.90 (m, 2H),

6.89 - 6.84 (m, 2H), 6.68 (s, 1H), 3.79 - 3.65 (m, 7H), 3.10 - 3.03 (m, 4H); HRMS calcd for $C_{29}H_{25}ClN_3O_6$ ([M - H]$^-$): 546.1437, found: 546.1432.

(*E*)-3-(5-(5-chloro-2,4-dihydroxyphenyl)-4-(4-hydroxyphenyl)isoxazol-3-yl)-1-(4-(3-methoxyphenyl)piperazin-1-yl)prop-2-en-1-one (**11c**). Compound **11c** was prepared according the described procedure of **11a**, to give **11c** as yellow solid (29.0 mg, 59% yield, HPLC purity: 97); mp 233 – 236 ^{o}C; ^{1}H NMR (400 MHz, Acetone-d_6) δ 7.39 (d, J = 15.6 Hz, 1H), 7.23 (m, 1H), 7.18 - 7.11 (m, 4H), 6.92 - 6.88 (m, 2H), 6.65 (s, 1H), 6.57 (dd, J = 8.2, 2.3 Hz, 1H), 6.52 (t, J = 2.3 Hz, 1H), 6.42 (dd, J = 8.1, 2.4 Hz, 1H), 3.77 - 3.63 (m, 7H), 3.22 - 3.15 (m, 4H); HRMS calcd for $C_{29}H_{25}ClN_3O_6$ ([M - H]$^-$): 546.1437, found: 546.1432.

(*E*)-3-(5-(5-chloro-2,4-dihydroxyphenyl)-4-(4-hydroxyphenyl)isoxazol-3-yl)-1-(4-(pyridin-2-yl)piperazin-1-yl)prop-2-en-1-one (**11d**). Compound **11d** was prepared according the described procedure of **11a**, to give **11d** as yellow amorphous solid (28.0 mg, 60% yield, HPLC purity: 100); ^{1}H NMR (400 MHz, Acetone-d_6) δ 8.16 (m, 1H), 7.56 (m, 1H), 7.42 (d, J = 15.6 Hz, 1H), 7.28 - 7.13 (m, 4H), 6.95 - 6.90 (m, 2H), 6.85 (d, J = 8.6 Hz, 1H), 6.71 - 6.64 (m, 2H), 3.78 - 3.56 (m, 8H); HRMS calcd for $C_{27}H_{22}ClN_4O_5$ ([M - H]$^-$): 517.1284, found: 517.1279.

(*E*)-3-(5-(5-chloro-2,4-dihydroxyphenyl)-4-(4-hydroxyphenyl)isoxazol-3-yl)-1-(4-(pyrimidin-2-yl)piperazin-1-yl)prop-2-en-1-one (11e). Compound **11e** was

prepared according the described procedure of **11a**, to give **11e** as yellow solid (26.2 mg, 56% yield, HPLC purity: 96); mp 248 – 250 °C; ^{1}H NMR (400 MHz, Acetone-d_6) δ 8.37 (d, J = 4.7 Hz, 2H), 7.41 (d, J = 15.6 Hz, 1H), 7.25 (s, 1H), 7.20 - 7.14 (m, 3H), 6.94 - 6.89 (m, 2H), 6.66 (s, 1H), 6.63 (t, J = 4.7 Hz, 1H), 3.90 - 3.81 (m, 4H), 3.73 - 3.60 (m, 4H); HRMS calcd for $C_{26}H_{21}ClN_5O_5$ ([M - H]$^-$): 518.1237, found: 518.1231.

(*E*)-3-(5-(5-chloro-2,4-dihydroxyphenyl)-4-(4-hydroxyphenyl)isoxazol-3-yl)-1-(4-(3,4-dichlorophenyl)piperazin-1-yl)prop-2-en-1-one (11f). Compound **11f** was prepared according the described procedure of **11a**, to give **11f** as yellow amorphous solid (31.6 mg, 60% yield, HPLC purity: 97); ^{1}H NMR (400 MHz, Acetone-d_6) δ 7.43 - 7.36 (m, 2H), 7.24 (s, 1H), 7.19 - 7.14 (m, 4H), 6.99 (dd, J = 9.0, 2.9 Hz, 1H), 6.93 - 6.88 (m, 2H), 6.66 (s, 1H), 3.80 - 3.70 (m, 4H), 3.33 - 3.25 (m, 4H); HRMS calcd for $C_{28}H_{21}Cl_3N_3O_5$ ([M - H]$^-$): 584.0552, found: 584.0541.

(*E*)-3-(5-(5-chloro-2,4-dihydroxyphenyl)-4-(4-hydroxyphenyl)isoxazol-3-yl)-1-(4-(3-(trifluoromethyl)phenyl)piperazin-1-yl)prop-2-en-1-one (11g). Compound **11g** was prepared according the described procedure of **11a**, to give **11g** as yellow solid (30.0 mg, 57% yield, HPLC purity: 98); mp 106 – 110 °C ^{1}H NMR (400 MHz, Acetone-d_6) δ 8.88 (brs, 1H), 7.51 - 7.36 (m, 2H), 7.30 - 7.23 (m, 3H), 7.22 - 7.09 (m, 4H), 6.94 - 6.87 (m, 2H), 6.68 (s, 1H), 3.84 - 3.71 (m, 4H), 3.39 - 3.29 (m, 4H); HRMS calcd for $C_{29}H_{22}ClF_3N_3O_5$ ([M - H]$^-$): 584.1206, found: 584.1200.

Biological procedures

Assay of the inhibitory activity of compounds

The inhibitory activity of compounds on PDHK was determined by enzyme-linked immunosorbent assay (ELISA). The enzymes PDHK1, PDHK2, PDHK3 and PDHK4, and substrate PDHA1 with His6-tagged SUMO fusion proteins were expressed in E.coli and purified with nickel column. The reaction was carried out with immobilized substrate (PDHA1, 0.5 μg/well), and adding with enzyme (0.25 μg/well), ATP (10 μM) with or without different concentrations of compounds in 100 μL of buffer (50mM HEPES, 10 mM $MgCl_2$ and 1mM EGTA). After reaction, the plate was washed and primary antibody (p-PDHA1(S293), Abgent, China) was added and incubated for 1 h. Then, the plate was washed and secondary anti-rabbit antibody with HRP conjunction was added and incubated for 1 h. The color was developed with o-phenylenediamine, and the absorbance (OD490) was measure by microplate reader (SPECTRA MAX 190, Molecular Devices). The inhibitory activity was calculated as four-parameter method. In ATP competitiveness assay, various concentrations of ATP and compounds were added to the reaction system, the Lineweaver-Burk plot was developed by 1/V (1/OD) (shown in y-axis) and 1/ATP (shown in x-axis). *In vitro* inhibitory activity of compounds on HSP90 at was determined by fluorescence polarization using full-length HSP90 and geldanamycin-BODIPY.

Western blot analysis

Proteins were extracted with RIPA buffer containing protease inhibitors cocktail. Equal total proteins per well were loaded for separation. After electrophoresis, proteins were transferred to a nitrocellulose membrane, blocked with TBST containing 3% BSA for 1 h at room temperature, then added respective primary antibody (Abgent, China), and incubated for 2 h at room temperature. After washing, secondary antibody was added and incubated for 1 h at room temperature. Bands were developed by enhanced chemiluminescence (ECL) and scanned by the ImageQuant LAS4000 (GE healthcare).

High content analysis

After treatment, cells were fixed with 4% paraformaldehyde at room temperature for 15 min, and washed three times with PBS at room temperature for 10 min and incubated with blocking solution (PBS, 3% of BSA, 0.1% Triton-X 100) at room temperature for 30 min. Primary antibody anti-p-PDHA1(S293, 1:400 dilution, Abgent, China) or anti-pPDHA1(S232, 1:400 dilution, Abgent, China) in primary antibody diluent (PBS, 3% BSA, 0.1% Triton-X100) was added and incubated at 4°C for 1 h; cells were washed with PBST, incubated with secondary antibody at room temperature for 1 h (goat anti-rabbit Alexa Fluor 488), and washed three times with PBS at room temperature for 10 min. Images were obtained with a high content analyzer (In Cell Analyzer 2000, GE healthcare). Data was analyzed by the software

provided by the supplier. Cells were defined as positive cells and negative cells according the fluorescence intensity with above or below the averaged intensity.

Lactate measurement

NIC-H1299, A549, H460, HCT116 and MDA-MB-231 cells were treated with different concentrations of compound 11a and DCA for 12 hours in serum-free medium, the lactate production was measured by lactate assay kit (Biovision, CA, USA). Meanwhile, total proteins of cell lysates were collected and quantified for normalization of lactate release.

Oxygen consumption and extracellular acidification rate analysis

The XF96 extracellular flux analyzer (Seahorse Biosciences, MA, USA) is a fully integrated 96-well instrument that measures in real-time the uptake and release of oxygen and pH, coupled to fiber-optic waveguides. This technology is widely used to measure oxygen consumption rate (OCR) expressed in pmol/min and extracellular acidification rate (ECAR) expressed in mpH/min. In this experiment, cells were firstly pre-treated with different concentrations of compounds for 12 h, and then cells were subjected to the XF96 extracellular flux analyzer for the measurement of OCR and ECAR.

Reactive oxygen species measurement

Intracellular ROS production was measured by probe DCFH-DA (Beyotime, Jiangsu, China). Briefly, cells were collected and loaded with 5 μmol/L of DCFH-DA in fresh medium for 30 min, and then washed with PBS. The cells were then subjected to FASC for analysis of the fluorescence intensity (BD Biosciences, USA).

Cell proliferation

NCI-H1299 cells were plated at a density of 3000 cells each well in 96-well plates. Different concentrations of compound **11a** were added to the wells the following day, and control cells were treated with the vehicle dimethyl sulfoxide. After 72 h of treatment, the cell proliferation was determined by CCK8 kit according to the protocol (Beyotime, Jiangsu, China).

Statistical Analysis

Data are shown as Mean±SD. Prism 6.0 (GraphPad Inc.) was used to perform the One-way ANOVA for comparison between groups. *$p < 0.05$ is considered statistically significant.

AUTHOR INFORMATION

Corresponding Authors

Shen J, Tel.: +86 21 50806600-5407; Fax: +86 21 50807088; E-mail: jkshen@simm.ac.cn;

Geng M, Tel.: +86 21 50806072; Fax.: +86 21 50806072; E-mail: mygeng@simm.ac.cn;

Huang M, Tel.: +86 21 50806600-2413; Fax.: +86 21 50806072; E-mail: mhuang@simm.ac.cn.

ACKNOWLEDGMENT

This work was supported by the National Science and Technology Major Project of the Ministry of Science and Technology of China (No. 2012ZX09301001-007) and National Natured Science Foundation of China (No. 81202549); M.H. is a young scholar funded by the National Natural Science Foundation of China (No. 81222049) and the Pujiang Scholar Program Grant by the Shanghai Metropolitan Government (NO. 12PJ1410400).

NOTES

The authors declare no competing financial interest.

Supporting Information Available

Synthetic procedures and analytical data for compounds **4**, **5a-m**, **6-9**, **12** and **13**, copies of ^{1}H-NMR for all the compounds. This material is available free of charge via the Internet at http://pubs.acs.org.

REFERENCES

(1) Vander Heiden, M. G. Targeting cancer metabolism: a therapeutic window opens. *Nat. Rev. Drug Discov.* **2012**, 10, 671-684.

(2) (a) Koukourakis, M. I.; Giatromanolaki, A.; Sivridis, E.; Gatter, K. C.; Harris, A. L. Pyruvate dehydrogenase and pyruvate dehydrogenase kinase expression in non small cell lung cancer and tumor-associated stroma. *Neoplasia* **2005**, 7, 1-6. (b) Koukourakis, M. I.; Giatromanolaki, A.; Bougioukas, G.; Sivridis, E. Lung cancer: a comparative study of metabolism related protein expression in cancer cells and tumor associated stroma. *Cancer Biol. Ther.* **2007**, 6, 1476-1479.

(3) Wigfield, S. M.; Winter, S. C.; Giatromanolaki, A.; Taylor, J.; Koukourakis, M. L.; Harris, A. L. PDK-1 regulates lactate production in hypoxia and is associated with poor prognosis in head and neck squamous cancer. *Br. J. Cancer* **2008**, 98, 1975-1984.

(4) (a) Kim, J. W.; Tchernyshyov, I.; Semenza, G. L.; Dang, C. V. HIF-1-mediated expression of pyruvate dehydrogenase kinase: a metabolic switch required for cellular adaptation to hypoxia. *Cell Metab.* **2006**, 3, 177-185. (b) Papandreou, I.; Cairns, R.

A.; Fontana, L.; Lim, A. L.; Denko, N. C. HIF-1 mediates adaptation to hypoxia by actively downregulating mitochondrial oxygen consumption. *Cell Metab.* **2006**, 3, 187-197.

(5) (a) Kim, J. W.; Gao, P.; Liu, Y. C.; Semenza, G. L.; Dang, C. V. Hypoxia-inducible factor 1 and dysregulated c-Myc cooperatively induce vascular endothelial growth factor and metabolic switches hexokinase 2 and pyruvate dehydrogenase kinase 1. *Mol. Cell. Biol.* **2007**, 27, 7381-7393. (b) McFate, T.; Mohyeldin, A.; Lu, H.; Thakar, J.; Henriques, J.; Halim, N. D.; Wu, H.; Schell, M. J.; Tsang, T. M.; Teahan, O.; Zhou, S.; Califano, J. A.; Jeoung, N. H.; Harris, R. A.; Verma, A. Pyruvate dehydrogenase complex activity controls metabolic and malignant phenotype in cancer cells. *J. Biol. Chem.* **2008**, 283, 22700-22708.

(6) Hitosugi, T.; Fan, J.; Chung, T. W.; Lythgoe, K.; Wang, X.; Xie, J.; Ge, Q.; Gu, T. L.; Polakiewicz, R. D.; Roesel, J. L.; Chen, G. Z.; Boggon, T. J.; Lonial, S.; Fu, H.; Khuri, F. R.; Kang, S.; Chen, J. Tyrosine phosphorylation of mitochondrial pyruvate dehydrogenase kinase 1 is important for cancer metabolism. *Mol. Cell* **2011**, 44, 864-877.

(7) (a) Sutendra, G.; Michelakis, E. D. Pyruvate dehydrogenase kinase as a novel therapeutic target in oncology. *Front Oncol.* **2013**, 3, 38. (b) Michelakis, E. D.; Webster, L.; Mackey, J. R. Dichloroacetate (DCA) as a potential metabolic-targeting therapy for cancer. *Br. J. Cancer* **2008**, 99, 989-994. (c) Michelakis, E. D.; Sutendra, G.; Dromparis, P.; Webster, L.; Haromy, A.; Niven, E.; Maguire, C.; Gammer, T. L.;

Mackey, J. R.; Fulton, D.; Abdulkarim, B.; McMurtry, M. S.; Petruk, K. C. Metabolic modulation of glioblastoma with dichloroacetate. *Sci. Transl. Med.* **2010**, 2, 31ra34.

(8) (a) Morrell, J. A.; Orme, J.; Butlin, R. J.; Roche, T. E.; Mayers, R. M.; Kilgour, E. AZD7545 is a selective inhibitor of pyruvate dehydrogenase kinase 2. *Biochem. Soc. Trans.* **2003**, 31, 1168-1170. (b) Aicher, T. D.; Anderson, R. C.; Bebernitz, G. R.; Coppola, G. M.; Jewell, C. F.; Knorr, D. C.; Liu, C.; Sperbeck, D. M.; Brand, L. J.; Strohschein, R. J.; Gao, J.; Vinluan, C. C.; Shetty, S. S.; Dragland, C.; Kaplan, E. L.; DelGrande, D.; Islam, A.; Liu, X.; Lozito, R. J.; Maniara, W. M.; Walter, R. E.; Mann, W. R. (R)-3,3,3-Trifluoro-2-hydroxy-2-methylpropionamides are orally active inhibitors of pyruvate dehydrogenase kinase. *J. Med. Chem.* **1999**, 42, 2741-2746.

(9) Korotchkina, L. G.; Patel, M. S. Probing the mechanism of inactivation of human pyruvate dehydrogenase by phosphorylation of three sites. *J. Biol. Chem.* **2001**, 276, 5731-5738.

(10) Dutta, R.; Inouye, M. GHKL, an emergent ATPase/kinase superfamily. *Trends Biochem. Sci.* **2000**, 25, 24-28.

(11) Bellon, S.; Parsons, J. D.; Wei, Y.; Hayakawa, K.; Swenson, L. L.; Charifson, P. S.; Lippke, J. A.; Aldape, R.; Gross, C. H. Crystal structures of Escherichia coli topoisomerase IV ParE subunit (24 and 43 kilodaltons): a single residue dictates differences in novobiocin potency against topoisomerase IV and DNA gyrase. *Antimicrob. Agents Chemother.* **2004**, 48, 1856-1864.

(12) (a) Steussy, C. N.; Popov, K. M.; Bowker-Kinley, M. M.; Sloan, R. B., Jr.; Harris, R. A.; Hamilton, J. A. Structure of pyruvate dehydrogenase kinase. Novel folding pattern for a serine protein kinase. *J. Biol. Chem.* **2001**, 276, 37443-37450. (b) Kato, M.; Li, J.; Chuang, J. L.; Chuang, D. T. Distinct structural mechanisms for inhibition of pyruvate dehydrogenase kinase isoforms by AZD7545, dichloroacetate, and radicicol. *Structure* **2007**, 15, 992-1004.

(13) (a) Biamonte, M. A.; Van de Water, R.; Arndt, J. W.; Scannevin, R. H.; Perret, D.; Lee, W. C. Heat Shock Protein 90: Inhibitors in Clinical Trials. *J. Med. Chem.* 2010, 53, 3-17. (b) Messaoudi, S.; Peyrat, J. F.; Brion, J. D.; Alami, M. Heat-shock protein 90 inhibitors as antitumor agents: a survey of the literature from 2005 to 2010. *Expert Opin. Ther. Pat.* **2011**, 21, 1501-1542.

(14) Kukimoto-Niino, M.; Tokmakov, A.; Terada, T.; Ohbayashi, N.; Fujimoto, T.; Gomi, S.; Shiromizu, I.; Kawamoto, M.; Matsusue, T.; Shirouzu, M.; Yokoyama, S. Inhibitor-bound structures of human pyruvate dehydrogenase kinase 4. *Acta Crystallogr. D. Biol. Crystallogr.* **2011**, 67, 763-773.

(15) Tuganova, A.; Yoder, M. D.; Popov, K. M. An essential role of Glu-243 and His-239 in the phosphotransfer reaction catalyzed by pyruvate dehydrogenase kinase. *J. Biol. Chem.* **2001**, 276, 17994-17999.

(16) Brough, P. A.; Aherne, W.; Barril, X.; Borgognoni, J.; Boxall, K.; Cansfield, J. E.; Cheung, K. M.; Collins, I.; Davies, N. G.; Drysdale, M. J.; Dymock, B.; Eccles, S. A.; Finch, H.; Fink, A.; Hayes, A.; Howes, R.; Hubbard, R. E.; James, K.; Jordan, A.

M.; Lockie, A.; Martins, V.; Massey, A.; Matthews, T. P.; McDonald, E.; Northfield, C. J.; Pearl, L. H.; Prodromou, C.; Ray, S.; Raynaud, F. I.; Roughley, S. D.; Sharp, S. Y.; Surgenor, A.; Walmsley, D. L.; Webb, P.; Wood, M.; Workman, P.; Wright, L. 4,5-diarylisoxazole HSP90 chaperone inhibitors: potential therapeutic agents for the treatment of cancer. *J. Med. Chem.* **2008**, 51, 196-218.

(17) (a) Chang, S.; Yin, S. L.; Wang, J.; Jing, Y. K.; Dong, J. H. Design and synthesis of novel 2-phenylaminopyrimidine (PAP) derivatives and their antiproliferative effects in human chronic myeloid leukemia cells. *Molecules* **2009**, 14, 4166-4179. (b) Kaffy, J.; Pontikis, R.; Florent, J. C.; Monneret, C. Synthesis and biological evaluation of vinylogous combretastatin A-4 derivatives. *Org. Biomol. Chem.* **2005**, 3, 2657-2660. (c) Li, Y. W.; Liu, J.; Liu, N.; Shi, D.; Zhou, X. T.; Lv, J. G.; Zhu, J.; Zheng, C. H.; Zhou, Y. J. Imidazolone-amide bridges and their effects on tubulin polymerization in cis-locked vinylogous combretastatin-A4 analogues: synthesis and biological evaluation. *Bioorg. Med. Chem.* **2011**, 19, 3579-3584. (d) Ty, N.; Kaffy, J.; Arrault, A.; Thoret, S.; Pontikis, R.; Dubois, J.; Morin-Allory, L.; Florent, J. C. Synthesis and biological evaluation of cis-locked vinylogous combretastatin-A4 analogues: derivatives with a cyclopropyl-vinyl or a cyclopropyl-amide bridge. *Bioorg. Med. Chem. Lett.* **2009**, 19, 1318-1322. (e) Wright, S. W.; Harris, R. R.; Kerr, J. S.; Green, A. M.; Pinto, D. J.; Bruin, E. M.; Collins, R. J.; Dorow, R. L.; Mantegna, L. R.; Sherk, S. R.; et al. Synthesis, chemical, and biological properties of vinylogous hydroxamic acids: dual inhibitors of 5-lipoxygenase and IL-1 biosynthesis. *J. Med. Chem.* **1992**, 35, 4061-4068.

(18) McLaughlin, S. H.; Ventouras, L. A.; Lobbezoo, B.; Jackson, S. E. Independent ATPase activity of Hsp90 subunits creates a flexible assembly platform. *J. Mol. Biol.* **2004**, 344, 813-826.

(19) Chong, L. P.; Wang, Y.; Gad, N.; Anderson, N.; Shah, B.; Zhao, R. A highly charged region in the middle domain of plant endoplasmic reticulum (ER)-localized heat-shock protein 90 is required for resistance to tunicamycin or high calcium-induced ER stresses. *J. Exp. Bot.* **2014**, *in press*.

(20) Tuganova, A.; Popov, K. M. Role of protein-protein interactions in the regulation of pyruvate dehydrogenase kinase activity. *Biochem. J.* **2005**, 387, 147-153.

Table of Contents graphic.